

emerges, despite the difficulties of dating both shell and bone. Ironically, Site E is now one of the best dated archaeological sites in Cyprus.

Based on the test excavations, I tentatively conclude that both points of significance mentioned earlier are correct: Site E is the earliest site in Cyprus and it appears that pygmy hippopotami were indeed hunted. Whether or not these animals became extinct because of human intervention cannot be determined on the basis of limited excavations at one site, but the implications are intriguing. It is essential that additional research be undertaken before the site completely erodes into the Mediterranean Sea.

This project could not have been undertaken without the volunteer effort of several very motivated professionals, the encouragement of Dr V Karageorghis and the Cypriot Department of Antiquities, the support of Dr S Swiny and the Cyprus American Archaeological Research Institute, and the assistance of the Western Sovereign Base Archaeological Society (Royal Air Force, Akrotiri). Partial funding was provided by the Desert Research Institute through a grant from the National Science Foundation's Experimental Program to Stimulate Competitive Research (EPSCoR).

Received 8 January; accepted 29 April 1988.

1. Cherry, J. *Proc. Prehist. Soc.* **47**, 41-68 (1981).
2. Burleigh, R. & J. Clutton-Brock *J. Archaeol. Sci.* **7**, 385-388 (1980).
3. Sondaar, P., Sanges, M., Kotsakis, T. & deBoer, P. *Geobios* **19**, 17-25 (1986).
4. Stanley-Price, N. *Levant* **9**, 66-89 (1977).
5. Stanley-Price, N. *World Archaeol.* **9**, 27-41 (1977).
6. Faure, M., Guerin, C. & Sondaar, P. *Actes Symp. Paleont. Cuvier, Montebeliard* 157-183 (1983).
7. Boeschoten, G. & Sondaar, P. *Koninkl. Nederl. Akad. van Weter* **75**, 306-338 (1972).
8. Bate, D. *Geol. Mag.* **5**, 324-325 (1904).
9. Davis, S. *The Archaeology of Animals* (Yale, New Haven, 1987).
10. Reese, D. *Earth Sci.* **28**, 63-69 (1975).
11. Reese, D. *Expedition* **17**, 26-30 (1975).
12. Vogel, J., Fuls, A. & Visser, E. *Radiocarbon* **28**, 1133-1172 (1986).
13. Vogel, J. & Waterbolk, H. *Radiocarbon* **5**, 163-202 (1963).
14. Vogel, J. & Visser, E. *Radiocarbon* **23**, 43-80 (1981).

## A unique colour and polarization vision system in mantis shrimps

N. Justin Marshall

School of Biological Sciences, University of Sussex, Falmer, Brighton, Sussex BN1 9QG, UK

The apposition compound eyes of mantis shrimps (stomatopods) are divided into three sections, the dorsal and ventral hemispheres and the midband. Many ommatidia of both hemispheres, and all those in the midband, sample the same narrow band in space. The function of the morphologically distinct midband region is not clear, but new evidence suggests that it may be adapted in a unique manner for colour and polarization vision. A series of carotenoid colour filters screen the photopigment and potentially provide a tetrachromatic input for contrast-enhanced vision or true colour vision<sup>1</sup>. The filters are blocks of coloured droplets (red, orange, yellow, purple, pink or blue) within the rhabdoms of two rows of midband ommatidia. The arrangement of tiered microvilli in two other midband rows suggests that they provide a unique form of polarization vision.

In gonodactyloid stomatopods several rows of ommatidia in each hemisphere, and all six rows of midband ommatidia, view the same area in space (Fig. 1). It has been assumed since the work of Exner<sup>2</sup>, that upper and lower hemispheres operate together as a rangefinder within each eye, and that this helps to mediate the behaviour for which stomatopods are famous: that is the ballistic smashing or spearing of prey with a pair of raptorial appendages. The midband does not readily fit this scheme and has ommatidia that are very different from those in the hemispheres<sup>3</sup>.

Figure 2 summarizes the internal structure of the midband

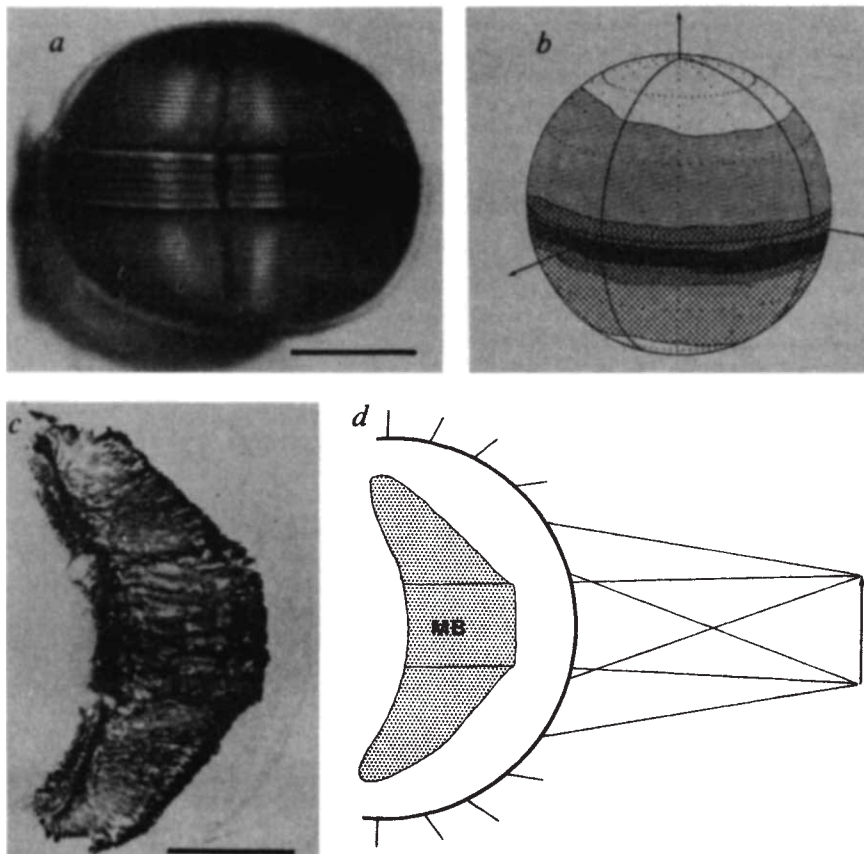


**Fig. 1** *a*, The eye of *Odontodactylus scyllarus* showing dorsal and ventral hemispheres and the six ommatidial rows in the midband, typical of gonodactyloid stomatopods. The enlarged facet diameter of the midband suggests a functional difference. The three vertical dark areas (the pseudopupils) are those areas of the eye looking at the observer. Scale, 1.5 mm. *b*, Field of view of the hemispheric and midband regions mapped on to an imaginary globe in space with the eye at the centre and arranged with the midband congruent to the equator. Measurements were made by mapping the pseudopupil position with a goniometer<sup>28</sup>. Small dots, top hemisphere; large dots, bottom hemisphere; solid shading, midband. Note the strip in space where the fields of view of all three areas overlap. In *O. scyllarus*, this strip subtends a maximum angle of 5-15°, but as this method tends to overestimate, the true value could be less. *c*, Sagittal cryosection of eye in *Gonodactylus ternatensis*. Note the amount of space the six midband rows occupy in the retina (the dark crescent) compared to the two hemispheres, each of which contains over 30 ommatidial rows. *d*, Diagram of the visual axes of the column of ommatidia shown in *c*, MB represents the midband region. The visual overlap of the three eye regions is due to ommatidial 'skewing' in each hemisphere towards the midband. The optical intersection of all three eye regions is not to scale.

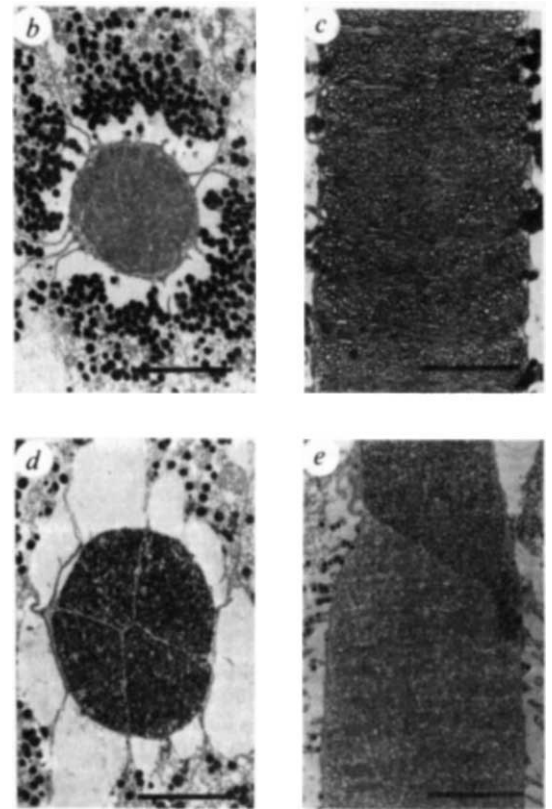
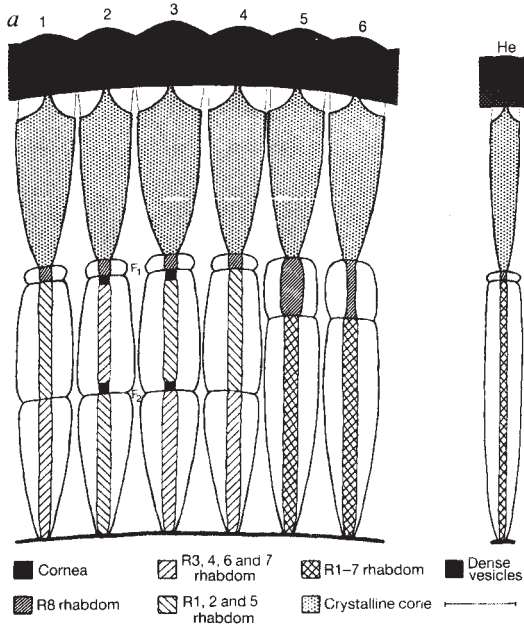


**Fig. 2** *a*, Schematic diagram of midband ommatidia in sagittal section for a gonodactyloid stomatopod; rows are labelled 1–6 dorsal–ventral (see Fig. 1). The rhabdom width is drawn as three times the actual width, and pigment cells are omitted for clarity. Note the tiered arrangement in all rhabdoms, in particular the two tiers in rows 2 and 3 labelled F1 and F2. The rhabdomeres contributing to each tier are indicated in the key and, apart from R8, follow no previous labelling system. Rows 5 and 6 are the subject of Fig. 4; however the relative length of R8 is shown here. A typical hemispheric ommatidium (He) is included for comparison. Scale, 150  $\mu\text{m}$ . *b*, Transmission electron micrograph (TEM) of the most proximal tier in midband row 3 of *G. chiragra* (transverse section). Note the four cells forming the rhabdom in this tier, R3, 4, 6 and 7. The three cells of the overlying tier, R1, 2 and 5, have formed axons. Scale, 6  $\mu\text{m}$ . *c*, TEM of midband row three, proximal tier in *G. chiragra*; longitudinal section. The layered, orthogonal arrangement of microvilli is typical of most crustaceans and is found in all stomatopod midband and hemispheric rhabdoms, including R8 cells, with the exception of the R8 tier in rows 5 and 6. Scale, 4  $\mu\text{m}$ . *d*, TEM of midband row 2 in *G. chiragra*, transverse section of F2 level; dense-staining vesicles are produced by R3, 4, 6 and 7 in place of rhabdom microvilli. Scale, 3  $\mu\text{m}$ . *e*, TEM of midband row 3 in *O. scyllarus*, longitudinal section of F2 and most proximal tier in row three. F1 and 2 tiers in rows 2 and 3 consist of densely staining vesicles that must filter light reaching more proximal layers. Scale, 5  $\mu\text{m}$ .

obtained from ultrathin and semithin serial sections. The rhabdoms of the lower and upper hemispheric regions are typical of many crustaceans and consist of eight reticular cells (R1–8) that are arranged in two tiers, with one cell (R8) producing the upper shorter layer (usually 5–10% of the total rhabdom length) and R1–7 producing the remainder<sup>4</sup>. Midband rhabdoms differ in three respects: (1) they are an average of 10% longer and 100% wider than those of the hemispheres; (2) rows 5 and 6 are two-tiered, like the ommatidia in the hemispheres, but the upper R8 layer is unusually long (20% of the total length) and both tier levels are unlike other rhabdoms in transverse section, being square at the R1–7 level and lozenge-shaped at the R8 level (Fig. 4); (3) there are three tiers in rows 1 and 4, and five in rows 2 and 3. Two of the tier levels in rows 2 and 3 are made up of electron-dense vesicles (Fig. 2), rather than microvilli, and these vesicles contain carotenoid pigments. Thus, in these two rows rhabdom blocks alternate with colour filters.

More than two retinal tiers have not been reported for any other crustacean; but some insects, butterflies and dragonflies for instance, have three-layered retinæ in at least a subsection of their eyes<sup>5,6</sup>. A possible function of such an arrangement is to assist in colour vision<sup>7</sup>. All colour vision systems studied to date (in both vertebrates and invertebrates) use multiple photopigments with different spectral sensitivities. Each photopigment is found in discrete receptor populations, and colour opponency is set up by comparison between the receptor types. Where tiered rhabdoms occur, one block of rhabdom is screened by the photopigment of another, and this filter action sharpens the spectral peak of the more proximal rhabdom, potentially improving the contrast between colours<sup>8</sup>.

Some vertebrates use another type of filter that has photostable coloured oil droplets positioned over the retinal cones<sup>9,10</sup>, so that light must pass through these before reaching the photopigment. The pigeon, for instance has red, yellow, green and clear droplets in its eye distributed in specific areas of its retina. The colouring in these structures comes from carotenoid pigments<sup>11</sup>, and with two or more differently coloured droplets acting as filters, it would in principle be possible to achieve colour vision with a single photopigment<sup>10</sup>. All animals with oil droplets so far examined, however, possess several photopigments, and retain colour vision even if the droplets are bleached of colour<sup>12</sup>. Birds may use these filters either to sharpen their existing spectral sensitivities or to divide the retina into areas with which to perform different visual tasks, such as distinguishing foliage or looking through water surfaces<sup>13</sup>.

The electron-dense droplet structures in stomatopods are very much larger than vertebrate oil droplets (Fig. 3). In cryosection they appear brightly coloured (red, yellow, orange, pink and, most surprisingly, blue and purple) and, from the three-peaked spectral characteristics, these pigments are likely to be carotenoids (Fig. 3)<sup>14</sup>. They are situated at two specific levels in all rhabdoms of rows 2 and 3 of the midbands: F1 and F2 in Fig. 2. Interestingly, the combination of colours at the F1 and F2 level have so far proved to be species-specific and may relate to body colouration. Most stomatopods are found on coral reefs and, like many tropical reef species, can be brightly coloured; *Odontodactylus scyllarus*, for instance, has striking red, yellow and blue markings on a predominantly green body. *Gonadactylus* sp. are often drab greens and browns, but possess brightly coloured meral spots on the inner surface of their



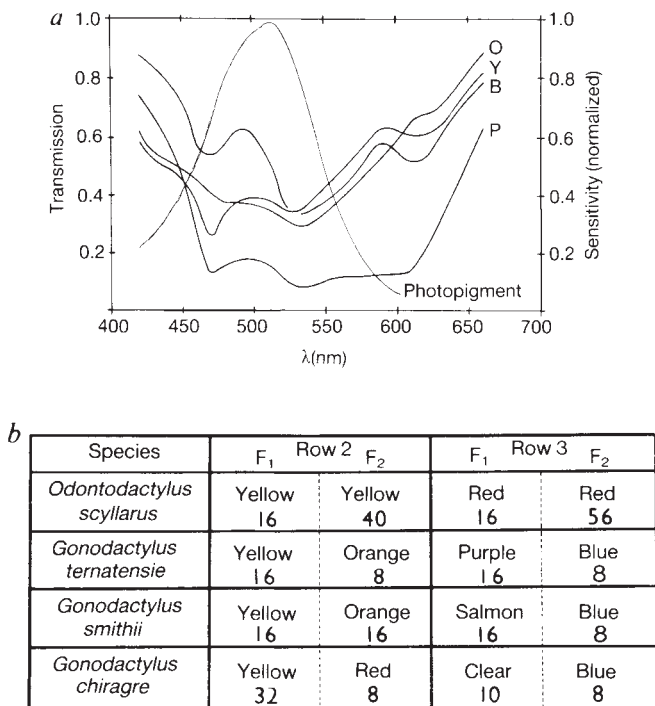


**Fig. 3** *a*, Transmission spectra of the four carotenoid filter blocks in *G. ternatensis*, the absorbance of which is corrected for relative filter length: O, orange; Y, yellow; B, blue and P, purple. Measurements were made using a microscope modified as a microspectrophotometer<sup>29</sup>. Normalized sensitivity spectrum of the photopigment probably present in R1-7 of the midband<sup>19</sup> is represented by the thin line. With such a combination, tetrachromatic vision is possible. *b*, Summary of filter colours at the F<sub>1</sub> and F<sub>2</sub> level in some species studied to date. Such filters are only found in rows 2 and 3 and their combination seems to be species specific. Also the length of the filters, and therefore the amount of light they let through to successive layers, varies between species. Average lengths in microns of filter blocks are given for 10-cm-long individual of each species.

raptorial appendages. These seem to be the only visible means of species identification and animals display these spots in inter- and intraspecific communication<sup>15</sup>. Species identification may be a function of ommatidial rows 2 and 3, and this would imply that the filters are concerned with true colour vision rather than contrast enhancement.

Amongst other arthropods, red pigment granules have been found in the retinae of some pierid butterflies, but most of this pigment is outside the rhabdom, where it could exert only a lateral filtering effect on the photopigment present<sup>16</sup>. In several species of fly, certain R7 rhabdomeres contain a photostable carotenoid pigment distributed in a diffuse manner within the microvillar portion of the cell<sup>17</sup>; here it may protect the R7 microvilli against photooxidation or shift the maximal spectral sensitivity of the underlying R8 cell<sup>18</sup>. The carotenoid pigment of stomatopods forms dense plugs situated in the rhabdom and must therefore act as a filter, altering the spectral quality of light reaching more proximal layers. As the length of the filters varies within and between species (Fig. 3), the strength of this effect will vary.

It is not clear at present whether or not stomatopods use several photopigments, like vertebrates. It is quite possible that they may achieve colour vision with a single photopigment. In most crustaceans, including stomatopods, one photopigment peaking at around 510 nm has been found in R1-7 (ref. 19). Recently Cummins and Goldsmith<sup>20</sup> demonstrated a violet-sensitive 440-nm photopigment in crayfish that is confined to the short distal R8 cells, and this may be the case for R8 cells

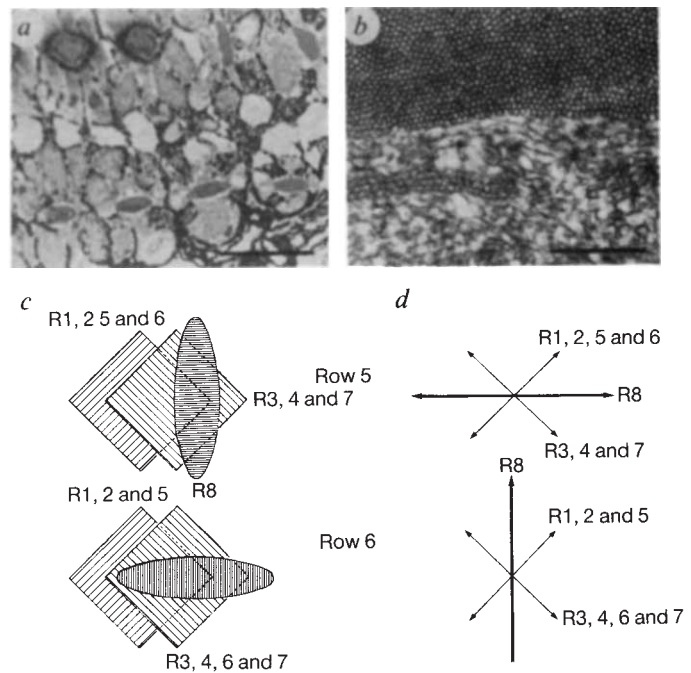


**Fig. 4** *a*, Semithin transverse section of midband rows 5 (top) and 6 in *O. scyllarus*: a cross-section taken to show both R8 and R1-7 rhabdom tier levels (R1-7 visible in row 5 only). R8 and R1-7 are both unusual in cross-section, being lozenge and rhombus-shaped respectively. Scale, 40  $\mu$ m. *b*, TEM of longitudinal section at R8/R1-7 join in *O. scyllarus*. Note the regular closely packed microvilli of R8 running in a single direction only and perpendicular to the lozenge long axis in *a*, which is typical of known polarization vision systems<sup>24</sup>. R1-7 microvilli are orthogonally arranged in that two groups of reticular cells carry microvilli perpendicular to each other. Scale, 1  $\mu$ m. *c*, Diagram of E-vectors, maximally absorbed in the complete rhabdom, showing single-direction R8 on top of orthogonal R1-7. Microvillus arrangement is shown on the left-hand side, and probable maximal sensitivity on the right. These directions do not change from ommatidium to ommatidium, nor do the individual ommatidia twist. The R8 cells (heavy arrows) may be part of a two-channel system with output comparison between rows 5 and 6. Alternatively, each of rows 5 and 6 may contain a separate three-channel system with output comparison: in row 6 for instance, between R8, R1, 2 and 5 and R3, 4, 6 and 7. Interestingly R8 cells are thought to contain short-wavelength photopigment (around 440 nm), and in many animals polarization sensitivity is greatest at this end of the spectrum<sup>30</sup>.

in other crustacean species<sup>21</sup>. Where the R8 cell is short, it will probably have little effect on the spectral sensitivity of the main R1-7 rhabdom tier. Stomatopods possessing two or more differently coloured carotenoid filters could construct a colour vision system based on a 510-nm photopigment in R1-7. Microspectrophotometry of the carotenoid filters (Fig. 3) indicates that they act as highly specific cutoff filters, restricting the spectral range of light incident on more proximal layers to long and short wavelengths (a rough indication of the resulting sensitivities would be the product of the transmission curves and sensitivity curve in Fig. 3). Rhabdomeres in midband rows 1 and 4, which have no carotenoid filters, might be compared against rows 2 and 3 to provide colour opponency at the neuronal level.

The structure of the remaining midband rows 5 and 6 strongly suggests that they operate as polarization analysers (Fig. 4). In many arthropods, polarization vision is thought to be based on rhabdomere structure, with most rhabdoms being maximally sensitive to light whose E-vector is parallel to the microvilli they carry<sup>22</sup>. Crustacean microvilli are typically arranged

orthogonally in alternating layers<sup>3</sup> (Fig. 2c), and in these a two-channel system could be envisaged, with the two rhabdomere subsets being most sensitive to light with E-vectors at right angles to each other. Labhart has recently demonstrated such a system in the dorsal rim area of crickets where rhabdom microvilli are also arranged orthogonally<sup>23</sup>.

R8 in rows 5 and 6 have microvilli arranged in one direction only and at right angles to each other. This suggests a two-channel system involving signal comparison between R8 cells in rows 5 and 6 (Fig. 4). Interestingly, R8 cells in these two rows are longer than in the rest of the eye and possess closely packed highly regular microvilli of the sort used in some known polarization vision systems<sup>24</sup>. They may therefore have a substantial polarizing effect on light reaching R1-7. It is possible that gonodactyloid stomatopods actually use two different three-channel systems. The rhabdom tier beneath R8, R1-7, in both rows 5 and 6, contains orthogonal microvilli whose two directions of maximal sensitivity are at 45° to those of R8. Comparison of three channels (R8; R1, 2 and 5 and R3, 4, 6 and 7 in row 6 ommatidia + R8; R1, 2, 5 and 6 and R3, 4 and 7 in row 5, see Fig. 4) eliminates the possible points of ambiguity found in a two-channel system<sup>25</sup>. This would allow a more accurate appraisal of polarized light in the environment. In stomatopods polarization vision might be involved in the analysis of shiny surfaces or particle-scattered light<sup>1</sup>. In both cases this may help increase the contrast with the background of objects being examined, such as potential predators or prey.

It seems likely that some stomatopods possess a potentially complex colour and polarization vision system in the midband region of their eyes. Before this can be stated with any certainty however, some behavioural evidence is needed to show positive discrimination between colours and between E-vectors. Such colour or polarization vision systems involving sequential filtering reduce the light reaching the rhabdom and the large lenses, and rhabdoms of the midband evidently compensate for this by increasing the light-gathering capabilities of the ommatidia. The narrow 'trinocular' strip viewed by each eye is moved through space by complex, largely independent eye movements<sup>26</sup> so that it may be swept over an object which the midband analyses for colour and polarization properties, and the two hemispheres for distance. Like many arthropods<sup>27</sup>, stomatopods have come up with an ingenious series of compromises and modifications to different areas of their eyes to perform different tasks.

Many thanks to Professor M. F. Land for invaluable tuition, guidance and criticism. Also thanks to Dr T. S. Collett and Dr R. C. Hardie for useful discussion and criticism, and to Dr J. R. Thorpe for technical advice. This study was supported by a grant from the SERC (UK).

Received 14 March; accepted 29 April 1988.

1. Lythgoe, J. N. *The Ecology of Vision* (Clarendon, Oxford, 1979).
2. Exner, S. in *Die Physiologie der Facettierten Augen von Krebsen und Insecten* (Deuticke, Leipzig and Wien, 1891).
3. Schiff, H. *Biol. Bull.* **170**, 461-480 (1986).
4. Waterman, T. H. in *Identified Neurons and Behaviour of Arthropods* (ed. Hoyle, G.) 317-386 (Plenum, New York, 1977).
5. Laughlin, S. B. & McGinness, S. *Cell Tiss. Res.* **188**, 427-447 (1978).
6. Schlecht, P. et al. *J. comp. Physiol.* **123**, 239-243 (1978).
7. Meinertzhagen, I. A. et al. *J. comp. Physiol.* **151**, 295-310 (1983).
8. Bowmaker, J. K. *Trends neuro. Sci.* **6**, 41-43 (1983).
9. Jane, S. D. & Bowmaker, J. K. *J. comp. Physiol.* **A162**, 225-235 (1988).
10. Bowmaker, J. K. *Trends neuro. Sci.* **3**, 196-199 (1980).
11. Liebman, P. A. & Granada, A. M. *Nature* **253**, 370-372 (1975).
12. Wallman, J. in *Neuronal Mechanisms of Behaviour in the Pigeon* (eds Granada, A. M. & Maxwell, J. H.) 327-351 (Plenum, New York, 1979).
13. Munz, W. R. A. in *Handbook of Sensory Physiology* Vol. VII/1 (ed. Autrum, H.) 529-565 (Springer, Berlin, 1972).
14. Fox, H. M. & Vevers, G. in *The Nature of Animal Colours* 62-80 (Sidgwick & Jackson, London, 1966).
15. Caldwell, R. L. & Dingle, H. *Scient. Am.* **234**, 80-89 (1976).
16. Ribi, W. A. *J. comp. Physiol.* **132**, 1-9 (1979).
17. Kirschfeld, K. et al. *J. comp. Physiol.* **125**, 275-284 (1978).
18. Kirschfeld, K. et al. *J. comp. Physiol.* **162**, 421-433 (1988).
19. Cronin, T. W. *J. comp. Physiol.* **156**, 679-687 (1985).
20. Cummins, D. R. & Goldsmith, T. H. *J. comp. Physiol.* **142**, 199-202 (1981).
21. Martin, F. G. & More, M. I. *J. comp. Physiol.* **145**, 549-554 (1982).
22. Snyder, A. W. & Laughlin, S. B. *J. comp. Physiol.* **100**, 101-166 (1975).

23. Labhart, T. *Nature* **331**, 435-437 (1988).
24. Saibil, H. & Hewat, E. *J. cell. Biol.* **105**, 19-28 (1987).
25. Bernard, G. D. & Wehner, R. *Vision Res.* **17**, 1019-1028 (1977).
26. Cronin, T. W. *J. expl. Biol.* (in the press).
27. Land, M. F. in *Facets of Vision* (ed. Hardie, R. C. & Stavenga, D. G.) (Springer, Berlin, in the press).
28. Horridge, G. A. *Phil. Trans. R. Soc.* **285**, 1-59 (1978).
29. Knowles, A. & Dartnall, H. J. in *The Eye* Vol. 2B (ed. Davson, H.) (Academic, London and New York, 1977).
30. Wehner, R. *J. comp. Physiol.* **161**, 511-531 (1987).

## Platelet-derived growth factor promotes division and motility and inhibits premature differentiation of the oligodendrocyte/type-2 astrocyte progenitor cell

Mark Noble\*§, Kerren Murray†, Paul Stroobant\*, Michael D. Waterfield\* & Peter Riddle‡

\* Ludwig Institute for Cancer Research, 91 Riding House Street, London W1P 8BT, UK

† Institut Merieux, 69260 Charbonniers les Bains, Lyon, France

‡ Imperial Cancer Research Fund, Lincoln's Inn Fields, London WC2A 3PX, UK

The mitogens which modulate cell-cell interactions during development of the central nervous system are unknown. One of the few interactions sufficiently well understood to allow identification of such molecules involves the two glial lineages which make up the rat optic nerve. One population of glial cells in this tissue, the type-1 astrocytes<sup>1</sup>, secrete a soluble factor(s) which promotes division of a second population of bipotential oligodendrocyte/type-2 astrocyte (O-2A) progenitor cells<sup>2</sup>; these progenitors give rise to oligodendrocytes, which myelinate large axons in the CNS, and type-2 astrocytes, which enwrap bare axons at nodes of Ranvier<sup>3,4</sup>. Type-1 astrocytes also promote progenitor motility<sup>5</sup>, and inhibit the premature differentiation of progenitors into oligodendrocytes which occur when these cells are grown in the absence of type-1 astrocytes<sup>2,3</sup>. We have now found that platelet-derived growth factor mimics the effects of type-1 astrocytes on O-2A progenitor cells, and antibodies to PDGF block the effects of type-1 astrocytes.

To analyse the molecular basis for the effects of type-1 astrocytes, we first looked at the ability of diverse growth factors (epidermal growth factor, basic fibroblast growth factor, transforming growth factor- $\alpha$ , transforming growth factor- $\beta$ , glial growth factor, platelet-derived growth factor and interleukins 1, 2 and 3) to modulate DNA synthesis and differentiation of O-2A progenitor cells in cultures derived from optic nerves of 7-day-old rats. Such cultures contain many O-2A progenitors, but few type-1 astrocytes, reducing the possibility that any effects might be indirectly mediated by type-1 astrocytes<sup>2,3</sup>. Individual cell-types were identified as described (refs 1-5; legend to Table 1). Only platelet-derived growth factor (PDGF) was found to mimic the effects of type-1 astrocytes.

PDGF promoted DNA synthesis in O-2A progenitor cells as effectively as type-1 astrocytes or astrocyte-conditioned medium (ACM) (Table 1). In the presence of 10 ng ml<sup>-1</sup> PDGF, 70-80% of the O-2A progenitors in cultures of 7-day-old optic nerve were labelled with [<sup>3</sup>H] thymidine during a 20 h pulse. With the best PDGF preparations, the response was maximal at  $\leq 5$  pM PDGF (Fig. 1a). As all batches of PDGF examined gave maximal responses at  $\leq 10$  ng ml<sup>-1</sup>, we used this concentration in most experiments.

PDGF also inhibited the rapid differentiation of progenitor cells into oligodendrocytes that is otherwise seen when these

§ To whom correspondence should be addressed.